Chinese Journal of
POLYMER SCIENCE

RESEARCH ARTICLE

https://doi.org/10.1007/s10118-026-3861-9
Chinese J. Polym. Sci.

Wavelength-selective Tough and Recyclable Photochromic Hydrogels Based on Competitive UV Energy Harvesting for Specific UVB Detector

Ting Ye[a,†], Hai-Bo Xiang[a,†], Meng-Xia Huang[a], Zi-Yuan Zhang[a], Kai-Rong Zang[a], Hong Wang[a*], and Jian Chen[a,b*]

[a] *Key Laboratory of Theoretical Organic Chemistry and Functional Molecule of Ministry of Education, Hunan Provincial Key Laboratory of Controllable Preparation and Functional Application of Fine Polymers, School of Chemistry and Chemical Engineering, Hunan University of Science and Technology, Xiangtan 411201, China*
[b] *Sanya Institute of Hunan University of Science and Technology, Sanya 572024, China*

Electronic Supplementary Information

Abstract Ultraviolet B (UVB) radiation plays a dual role in human health by promoting vitamin D synthesis and causing skin and ocular damage upon excessive exposure. However, the development of specific visual UVB sensors remains challenging. Herein, we report tough and recyclable photochromic hydrogels (PHs) by integrating engineered photochromic nanoparticles, which contain a diarylethene derivative (DTE) and a UV absorber (Trz), into poly(vinyl alcohol) (PVA) hydrogels through a synergistic freeze-casting and salting-out strategy. Benefiting from the competitive UV absorption relationship between DTE and Trz, PHs exhibited selective responses to UVB while effectively suppressing interference from UVA. The photochromic nanoparticles exhibited a low UVB detection limit of 0.024 W/m^2, rapid and highly reversible photoswitching, excellent photofatigue resistance over multiple switching cycles, and outstanding thermal and storage stabilities. By regulating the Trz content, the response thresholds of the nanoparticles can be precisely programmed, enabling visually distinguishable and dose-dependent color transitions over different UVB exposure intervals. Moreover, the PHs exhibited excellent mechanical performance, with a tensile strength of up to 22.29 MPa, remarkable flexibility, load-bearing capability, and recyclability without noticeable degradation of mechanical properties. Finally, a wearable wristband assembled from multiple hydrogel sensing units with programmable response thresholds was fabricated, which converts cumulative UVB exposure into discrete and highly distinguishable color states corresponding to different minimum erythema dose (MED) levels. This strategy offers a new platform for multi-molecule-based UV sensing, with potential applications in personal photoprotection and environmental monitoring.

Keywords Ultraviolet B (UVB); Diarylethene; UV absorber; Polymer nanoparticles; Photochromic hydrogels

Citation: Ye, T.; Xiang, H. B.; Huang, M. X.; Zhang, Z. Y.; Zang, K. R.; Wang, H.; Chen, J. Wavelength-selective tough and recyclable photochromic hydrogels based on competitive UV energy harvesting for specific UVB detector. *Chinese J. Polym. Sci.* https://doi.org/10.1007/s10118-026-3861-9

INTRODUCTION

Ultraviolet B (UVB, 280–320 nm), a high-energy, yet shallowly penetrating component of solar radiation, exerts a dual impact on human health. Moderate UVB exposure is indispensable for cutaneous vitamin D synthesis, whereas excessive exposure can lead to sunburn, photocarcinogenesis, and ocular disorders.[1–7] The mutagenic and carcinogenic effects of UVB are largely attributed to its direct interaction with DNA, which underscores the need for reliable UVB detection and monitoring technologies. Photochromic polymer materials, which change color upon exposure to light, offer a lightweight and convenient approach to visualizing ultraviolet exposure and have attracted substantial interest for wearable and environmental sensing applications, as well as anti-counterfeiting technologies.[8–14] These materials are usually prepared by integrating photochromic molecules (*i.e.*, spiropyrans, azobenzenes, and diarylethenes) into the polymer matrix *via* doping or covalent bonding to enhance stability. Among the various photochromic compounds, diarylethene (DTE) derivatives undergo thermally irreversible switching between open- and closed-ring isomers while exhibiting exceptional photofatigue resistance, pronounced visible-light absorption modulation, and excellent cycling stability.[15–23] These characteristics make DTE one of the most promising photochromic platforms for durable optical sensing and information-storage applications. The key performance metrics of photochromic UV sensors, including spectral selectivity, optical contrast, reversibility, and long-term photostability, are governed not only by the intrinsic photophysical properties of the photochromic molecules, but also by their local microenvironment within the host matrix.[24–28] Therefore, designing effective UVB detectors requires careful selection and engineering of DTE-based photochromic molecules and host architec-

* Corresponding authors, E-mail: whgxily@gmail.com (H.W.)
E-mail: cj0066@gmail.com (J.C.)
† These authors contributed equally to this work.
Received August 11, 2026; Accepted August 25, 2026; Published online November 5, 2026

© Chinese Chemical Society
Institute of Chemistry, Chinese Academy of Sciences

tures to balance sensitivity, selectivity, mechanical compatibility, and operational durability for real-world wearable applications.

A major challenge in UV sensing is the spectral selectivity.[24,29,30] Many photochromic molecules respond to broad UV bands, making exclusive detection of UVB difficult.[17,22,24,29,31–34] Existing solutions typically rely on physical UVA filters or the incorporation of additional UVA-absorbing species to suppress unwanted responses; however, these approaches add complexity and can limit sensitivity or durability.[24,34] Furthermore, most photochromic systems exhibit single-mode color changes and limited environmental robustness, impeding accurate dose discrimination and long-term deployment under complex conditions.[24,29,33] Therefore, an important challenge is to integrate wavelength selectivity, graded dose-dependent optical responses, mechanical resilience, and long-term environmental stability within a single UV sensing platform.[29,35–40] Polymer nanoparticles offer a versatile route to encapsulate multiple functional molecules within nanoparticles, enabling the co-assembly of photochromic dyes and wavelength-selective absorbers while preserving the photoswitching performance.[10,28,41–45] Although polymer nanoparticles possess many advantages, such as simple preparation, customized coupled dyes, facile functionalization, uniform dispersion, and scalable processing, their poor mechanical properties still limit their application. In contrast, tough hydrogels composed of water and hydrophilic polymer networks provide a complementary route for integrating functional nanoparticles, while providing flexibility, structural tunability, and robust mechanical performance.[43,46–50]

Integrating engineered nanoparticles into a robust hydrogel matrix to develop wearable UVB sensors that deliver both precise spectral discrimination and the mechanical toughness required for practical use is desired.[43,51–53] Recently, some studies have demonstrated the potential of photoresponsive polymer and hydrogel systems for electronic-free and wearable optical sensing.[51,54–56] For example, self-healing photochromic elastomer composites have been developed for programmable UV dose monitoring, enabling skin-mounted textile-integrated wristband-type sensors.[56] Multifunctional ionic hydrogels have been explored for outdoor UV monitoring by combining UV responsiveness with mechanical robustness and environmental tolerance.[51] These advances highlight the advantages of integrating optical sensing functions directly into soft and deformable polymeric matrices. Nevertheless, most reported systems primarily focus on broad-spectrum UV responsiveness or multifunctionality, whereas achieving selective detection of a specific UV band together with graded dose-dependent optical output remains challenging. Therefore, the development of mechanically robust wearable hydrogels with wavelength-selective response is highly desirable.

Herein, we report tough and recyclable photochromic hydrogels (PHs) obtained by combining simple freeze-casting and salting out to integrate engineered photochromic nanoparticles containing diarylethene-based photochromic units (DTE) and UVB-specific absorbers (Trz) into poly(vinyl alcohol) (PVA) hydrogels. Polymer nanoparticles encapsulating DTE and Trz were synthesized using simple miniemulsion polymerization, and then embedded into PVA hydrogels *via* the synergy of simple freeze-casting and salting out to produce PHs. The as-prepared PHs exhibited the following advantages: (i) selective response to UVB with clear, dose-dependent color changes, (ii) suppressed interference from longer-wavelength UVA through competitive absorption, (iii) rapid, highly reversible photoswitching and long-term optical stability, and (iv) high mechanical strength, recyclability, and environmental robustness suitable for wearable devices. We demonstrated PHs as a wearable UVB monitor that provides graded, visually readable responses corresponding to different UVB doses. Wavelength- and dose-selective color patterns revealed hidden marks only under controlled ultraviolet B (UVB) exposure. The combination of engineered photochromic nanoparticles and tough hydrogel matrices yielded a versatile platform for precise UVB sensing.

EXPERIMENTAL

The experimental details are included in the electronic supplementary information (ESI).

RESULTS AND DISCUSSION

Design and Preparation of Nanoparticles

Fig. 1 shows the design of the concepts and applications. Considering the limited wavelength selectivity, poor dose discrimination, and insufficient mechanical robustness of conventional photochromic UV sensors, we proposed a hierarchical design strategy that integrates engineered photochromic nanoparticles with tough hydrogels (Fig. 1a). Specifically, a diarylethene derivative, 3,3'-(thiophene-2,3-diyl)bis(2-methylbenzo[*b*]thiophene) (DTE), possessing excellent photofatigue resistance and reversible photochromic properties, was selected as the UV-responsive unit, whereas a hydroxyphenyl triazine UV absorber (2-(4,6-diphenyl-1,3,5-triazin-2-yl)-5-(hexyloxy)phenol, Trz) was introduced as a spectral regulator to selectively modulate the UVB-triggered photochromic response of DTE (Fig. 1a). Owing to the substantial overlap between the UVB absorption bands of DTE and Trz, a competitive absorption mechanism was established, whereby Trz preferentially dissipates incident UV energy, and only excess UVB photons can activate the ring-closing reaction of DTE. By precisely regulating the Trz content, the UV response threshold and color evolution kinetics of DTE can be programmed, enabling the wavelength-selective and dose-resolved visual detection of UVB irradiation. To overcome the poor mechanical properties of polymer nanoparticles, DTE/Trz-loaded nanoparticles prepared *via* simple one-step miniemulsion polymerization were further embedded into PVA hydrogels through the synergistic effects of freeze-casting and salting-out. The resulting hydrogel network not only uniformly dispersed the functional nanoparticles, but also provided excellent mechanical strength, flexibility, environmental stability, and recyclability through extensive interchain hydrogen-bond interactions. Finally, by integrating multiple hydrogel sensing units with programmable response thresholds into a wearable platform, cumulative UVB exposure can be transformed into discrete and visually distinguishable color states corresponding to different minimum erythema dose (MED) levels (Fig. 1b), thereby realizing high-resolution, reusable, and wearable UVB moni-

https://doi.org/10.1007/s10118-026-3861-9

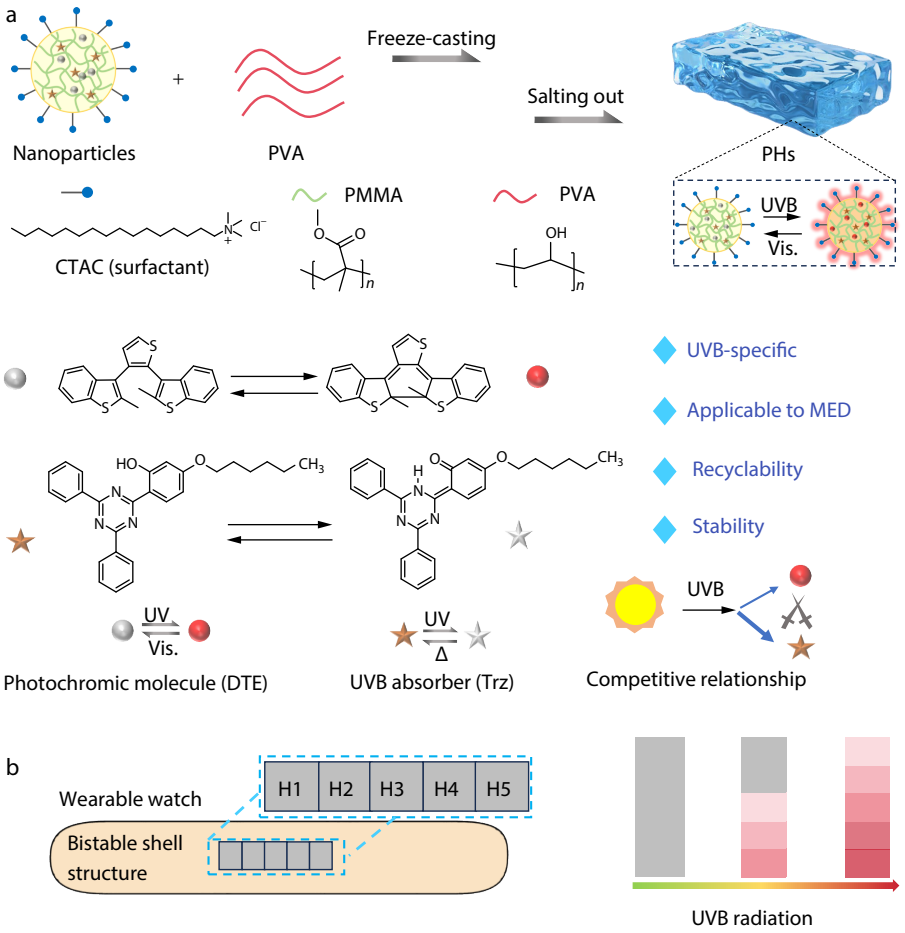


Fig. 1 Conceptual scheme of tough and recyclable PHs. (a) Schematic diagram of preparation process of PHs and the corresponding molecular structure (hexadecyl trimethyl ammonium chloride (CTAC), poly(methyl methacrylate) (PMMA), poly(vinyl alcohol) (PVA)), photoisomerization process of DTE (photochromic molecule) and Trz (UVB absorber), competitive relationship between DTE and Trz, and advantages. The photoisomerization process of DTE results in a color change from colorless to red, while Trz does not involve any color change process. In the competitive relationship between DTE and Trz, the UVB absorbility of Trz is stronger than DTE. (b) Schematic illustration of UV detection application (UV detection wristband) and corresponding color change under UVB irradiation.

toring.

Photochromic DTE was synthesized according to a previously reported method.[22] The detailed synthetic route is presented in Fig. S1 (in ESI), while the corresponding nuclear magnetic resonance (NMR) spectra and solvent-dependent spectral characterizations are shown in Figs. S2–S4 (in ESI), respectively. Trz exhibited no obvious photoresponsive characteristics in different solvents (trichloromethane ($CHCl_3$), dichloromethane (DCM), *N*,*N*-dimethylformamide (DMF), ethyl acetate (EA), *n*-hexane (Hex), ethyl acetate (EA), tetrahydrofuran (THF), Fig. S5 in ESI) because of its rapid thermal recovery property. Trz can undergo fast and reversible excited-state intramolecular proton transfer (ESIPT) under UV irradiation and is stored in the dark (Fig. 1a).[57] Spectral selectivity, that is, the ability to distinguish different UV wavelengths, is a critical criterion for evaluating the practical applicability of UV sensors. However, most reported UV sensors exhibit limited spectral discrimination and are susceptible to interference from nontarget UV wavelengths. Therefore, the spectral properties of DTE in dichloromethane (DCM) were first investigated. DTE underwent an intramolecular ring-closing reaction upon irradiation with UV light (254 nm (1 mW/cm^2) and 302 nm (100 μW/cm^2)), leading to the appearance of a characteristic absorption peak at 536 nm (Figs. S6a and S6b in ESI). In contrast, UVA (365 nm (15 mW/cm^2)) did not induce any noticeable increase in the absorption peak at 536 nm and no obvious color change was observed (Fig. S6c in ESI). Moreover, the UV absorption band of the DTE significantly overlapped with that of the UV absorber (Trz, Fig. S6d in ESI). These results indicate that DTE presented negligible responsiveness toward the UVA region and was essentially unaffected by UVA irradiation. Interestingly, DTE and Trz display a high degree of spectral overlap within the UVB region, providing a feasible strategy for regulating the UV detection range by tuning the competitive absorption relationship between DTE and Trz. The distinct spectral responses of DTE and Trz establish a solid foundation for constructing nanoparticles with tunable wavelength-selective photoresponses.

As illustrated in Fig. 2(a), the synthesis procedure for the nanoparticles is schematically depicted. DTE and Trz were co-encapsulated into polymer nanoparticles through facile one-pot miniemulsion polymerization of methyl methacrylate

https://doi.org/10.1007/s10118-026-3861-9

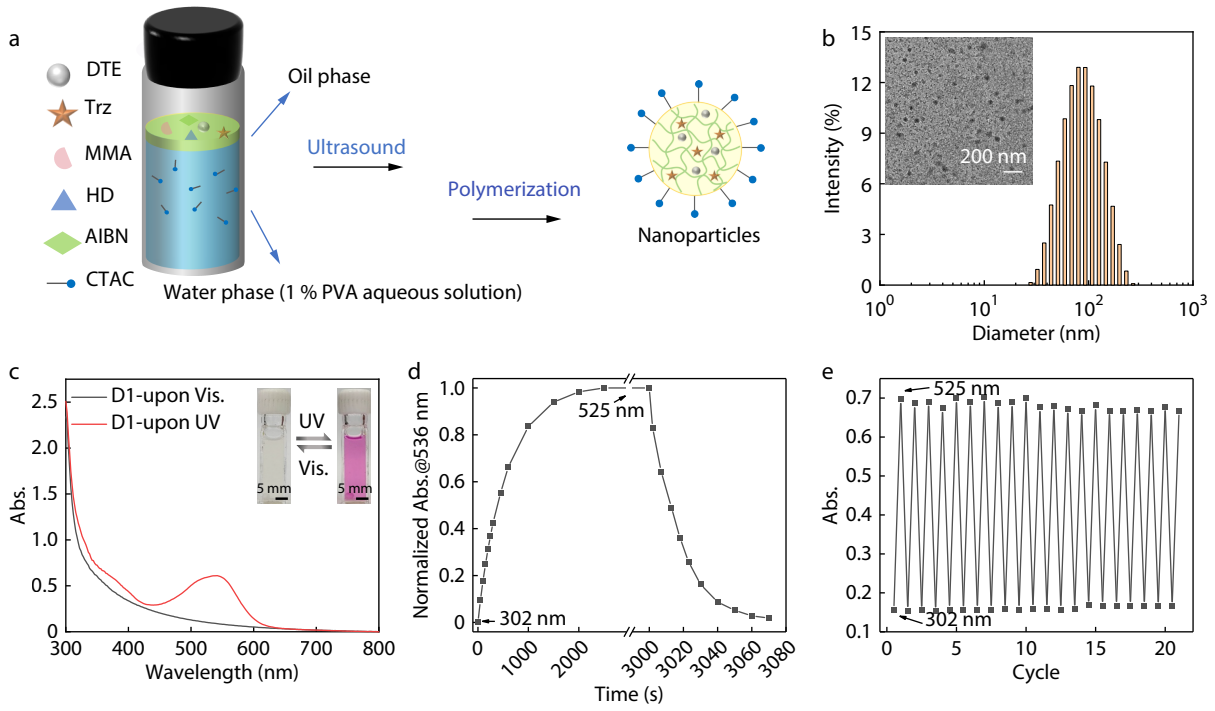


Fig. 2 (a) Schematic diagram of the preparation of nanoparticles and their constituent components; (b) DLS characterization of N1 sample. Inset in (b): TEM image. (c) Absorption spectra of N1 after UVB (302 nm, 100 μW/cm^2) irradiation. Inset in (c): optical photographs of N1 after UVB (302 nm, 100 μW/cm^2) or Vis. (525 nm, 1.34 mW/cm^2) irradiation. (d) The photo-responsiveness of N1 under UVB (302 nm, 100 μW/cm^2) and Vis. irradiation; (e) The switching cycles of N1 under alternative UVB and Vis. irradiation.

(MMA). The oil phase consisted of DTE, Trz, MMA, hexadecane (HD), and azobisisobutyronitrile (AIBN), whereas the aqueous phase was composed of a 1 wt% PVA and *N*-hexadecyltrimethylammonium chloride (CTAC) solution. To determine the optimal amount of DTE, nanoparticles containing 1, 3, 5, 7, and 9 mg of DTE were prepared (Table S1 in ESI). The color change of the nanoparticles under UVB irradiation was positively correlated with DTE content (Fig. S7 in ESI). Specifically, increasing the DTE concentration resulted in progressively darker coloration of the miniemulsion (nanoparticle solutions), and distinct color discrimination was observed when the DTE dosage reached 5 mg. Therefore, 5 mg of DTE (N1) was selected for the subsequent experiments.

For example, N1 was chosen as a typical sample to investigate the morphology using dynamic light scattering (DLS) and transmission electron microscopy (TEM). The results indicate that N1 has an average particle size of 65.28 nm with a narrow polydispersity index (PDI) of 0.188 (DLS, Table S1 in ESI, Fig. 2b) and show a dispersed, uniform, and spherical structure (TEM, 51.23 nm). As shown in Fig. 2(c), the absorption spectrum of N1 under alternating irradiation with UVB (302 nm, 100 μW/cm^2) and green light (525 nm, 1.34 mW/cm^2) was investigated. Upon UVB irradiation, the absorption peak of N1 at 536 nm gradually increased, accompanied by a distinct transition from colorless to deep red (Fig. 2c).

Understanding the photoswitchable characteristics of photochromic systems is essential for their practical applications. Therefore, the photoswitchable behavior and fatigue resistance of N1 were systematically investigated. In the initial state, the absorption intensity of N1 at 536 nm gradually increased under continuous irradiation with 302 nm UVB (100 μW/cm^2) and reached a maximum after 40 min. Subsequently, exposure to 525 nm visible light. (1.34 mW/cm^2) for 50 s caused the absorption intensity to rapidly decrease to its minimum value (Fig. 2d). In addition, when N1 was placed in an incandescent lamp, its absorption value decayed to colorless within 1000 s, which confirms that this molecule can complete the recovery process without the need for an external light source (such as green light), demonstrating its inherent spontaneous recovery characteristic (Fig. S8 in ESI). Furthermore, alternating irradiation with ultraviolet (UV) and visible light was used. was used to evaluate the photoreversibility of N1. As shown in Fig. 2(e), N1 retained a stable photoswitching behavior over more than 20 irradiation cycles without noticeable photobleaching, demonstrating excellent reversibility and fatigue resistance.

The stability of ultraviolet sensors ultimately determines their practical performance and service lifetime. Therefore, the long-term stability of the nanoparticles was evaluated. Only a slight increase in particle size was observed after storage for four weeks (Fig. S9 in ESI), indicating excellent colloidal stability. In addition, the optical stability of the nanoparticles under harsh conditions was investigated by monitoring their photochromic properties after storage at 60 °C and over prolonged storage periods. No significant deterioration in the photochromic performance was observed under either condition (Fig. S10 in ESI), demonstrating the excellent thermal and storage stability of these nanoparticles as ultraviolet sensing materials.

Characterization of Nanoparticles

A series of nanoparticles containing different amounts of Trz (0, 2.5, 5, 10, and 20 mg) was prepared. All samples exhibited a uniform particle size distribution (Table S1 in ESI). The maximum

https://doi.org/10.1007/s10118-026-3861-9

absorbance values of N1 and the corresponding linear fitting curves are shown in Fig. 3(a). Based on the evolution of the absorption peak, the absorbance of N1 gradually increased with increasing UVB dose and reached a maximum at an accumulated dose of 2000 J/m^2. These results demonstrate that the prepared nanoparticles exhibit a dose-dependent response to ultraviolet irradiation, confirming their feasibility as UV-sensing materials.

By analyzing the fitting curves of the absorption changes for each sample (Figs. 3b and 3c) and comprehensively considering both the extent of color variation and response sensitivity under low-intensity irradiation and different wavelengths (UVA, UVB, Fig. 3d, Fig. S11 in ESI), 5 loading was determined to be the optimal DTE mg. Under these conditions, the limit of detection (LOD) for UVB irradiation was calculated to be as low as 0.024 W/m^2, indicating excellent sensing performance. To ensure experimental consistency, all subsequent measurements were performed using a single UVB light source (100 μW/cm^2).

The color evolution of nanoparticles with different Trz contents under UV irradiation was further investigated (Fig. 3e). Distinct and highly reproducible color variations were observed as the UV dose was increased. Notably, the final coloration progressively became lighter with increasing Trz loading. This phenomenon can be attributed to the unique photophysical properties of the Trz. Upon UV absorption, the Trz molecules were excited from the ground state to the excited state, accompanied by hydrogen bond dissociation and molecular isomerization. The absorbed UV energy is rapidly dissipated as thermal energy through vibrational relaxation and internal conversion processes. Because these processes were reversible and did not induce any color change in Trz, increasing the Trz content effectively reduced the amount of UV energy available to activate the photochromic transition of the DTE. Therefore, the competitive UV absorption between Trz and DTE endowed the system with a threshold response. Only when the incident UV irradiation exceeded the absorption capacity of Trz could sufficient UV energy reach the DTE to trigger the ring-closing reaction, resulting in an observable color transition (Fig. S11 in ESI). This competitive absorption mechanism enabled the precise regulation of the photochromic response threshold.

Visual determination of cumulative UV doses has long been an important goal in the development of simple and user-interpretable ultraviolet dosimeters.[58,59] In this study, by integrating a UV absorber (Trz) with photochromic sensing molecules (DTE), real-time detection of different UVB dose intervals was successfully achieved. As shown in Figs. 3(e) and 3(f), the color evolution of nanoparticles N1–N5 under UV irradiation exhibited excellent resolution, and the coloring rate decreased linearly with increasing Trz loading (Fig. S12 in ESI). These results demonstrate that modulation of Trz content provides an effective strategy for constructing wavelength-selective and dose-resolved visual UVB sensors.

Characterization of PHs in Hydrogels

Although the nanoparticles exhibited excellent characteristics,

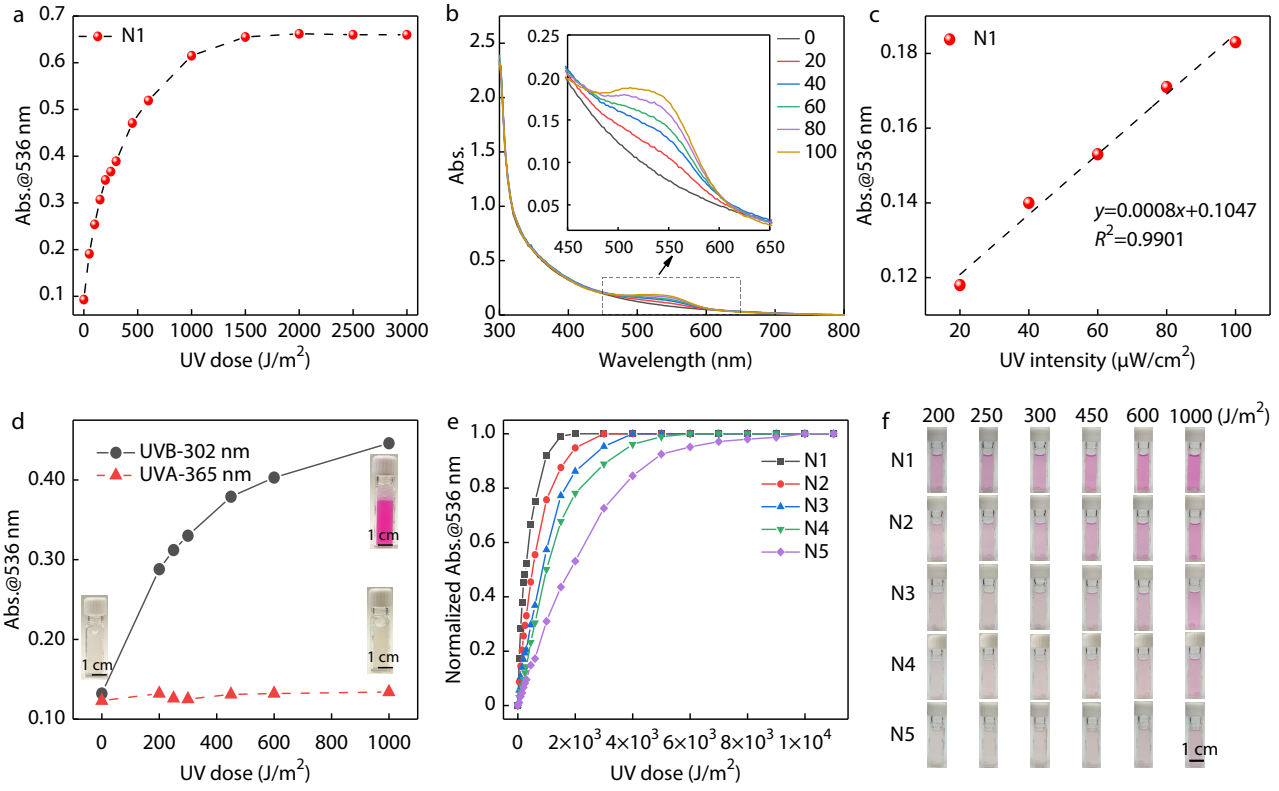


Fig. 3 (a) The absorbance of N1 at 536 nm with the change of UVB dose (J/m^2); (b) The absorption of N1 with different UVB intensity (0–100 μW/cm^2); (c) Relationship between the absorbance (536 nm) of N1 and UVB intensity; (d) The absorbance of N1 at 536 nm under 302 nm (UVB, 100 μW/cm^2) and 365 nm (UVA, 2.8 mW/cm^2) irradiation; (e) The absorbance change (536 nm) of N1, N2, N3, N4, and N5 under UVB irradiation (0–1.1×10^4 J/m^2), and (f) the corresponding photographs from 200 J/m^2 to1000 J/m^2.

https://doi.org/10.1007/s10118-026-3861-9

including high spectral selectivity, low detection limits, and facile functionalization, their poor mechanical robustness still limits their practical application of UV sensors. To address this issue, PVA was employed as a polymer matrix to fabricate nanoparticle-embedded tough hydrogels (PHs) through the synergy of simple freeze-casting and salting out (Fig. 4a).[43] The nanoparticles (N1) and PVA were dispersed in water to form a stable and highly viscous precursor solution (c_{N1}=2 wt% and c_{PVA}=18 wt%). The resulting solution was transferred into a glass mold with a spacing of 2 mm, frozen at –20 °C for 12 h, and subsequently thawed at 25 °C for 12 h. After three freeze-thaw cycles, the transparent hydrogel was immersed in a 1.5 M sodium citrate solution for one week, producing a hydrogel with a thickness of approximately 1 mm and a volume shrinkage of approximately 70%. The spatial distribution of the nanoparticles within the hydrogel matrix was evaluated by monitoring the color changes of the hydrogels (H1–H5, Table S2 in ESI) under UVB irradiation. The homogeneous photochromic response indicates that the nanoparticles were uniformly dispersed throughout the hydrogel network (Fig. 4b). Notably, incorporation of the nanoparticles into the hydrogel matrix did not compromise their photochromic performance, indicating that the hydrogel platform effectively preserved the UV-responsive properties of the nanoparticles and possessed great potential for wearable UVB-sensing applications.

Moreover, all hydrogel samples exhibited excellent mechanical performance, with a tensile strength as high as 22.29 MPa (Fig. 4c, Table S2 in ESI). The incorporation of polymer nanoparticles can slightly reinforce the hydrogel network by promoting additional physical interactions and energy-dissipation mechanisms.[43] The mechanical properties of the composite hydrogels were also evaluated. As shown in Fig. 4(d), PH1 could be twisted, knotted, bent, and stretched without fracture, and was even capable of lifting a bucket containing 5 kg of water, highlighting its remarkable toughness and load-bearing capability. Interestingly, the prepared PHs exhibit a characteristic lamellar structure consisting of transparent outer layers and an opaque middle region. To elucidate the origin of this unique morphology, cross-sections of freeze-dried and salt-treated H1 were characterized using scanning electron microscopy (SEM). The thicknesses of the upper layer, lower layer, and middle region were measured to be approximately 300.4, 174.3, and 236.9 μm, respectively (Fig. S13 in ESI).[43] The nanoparticle particles at the cross section can be clearly observed (Fig. S14 in ESI).

The outstanding mechanical performance of PVA hydrogels originates from the extensive interchain hydrogen bonding interactions among the PVA chains. These hydrogen bonds dissociated at elevated temperatures, endowing the hydrogel with excellent recyclability and reprocessability. To demonstrate this feature, a square-shaped H1 hydrogel (Fig. 4e) was first cut into small pieces. The fragments were then

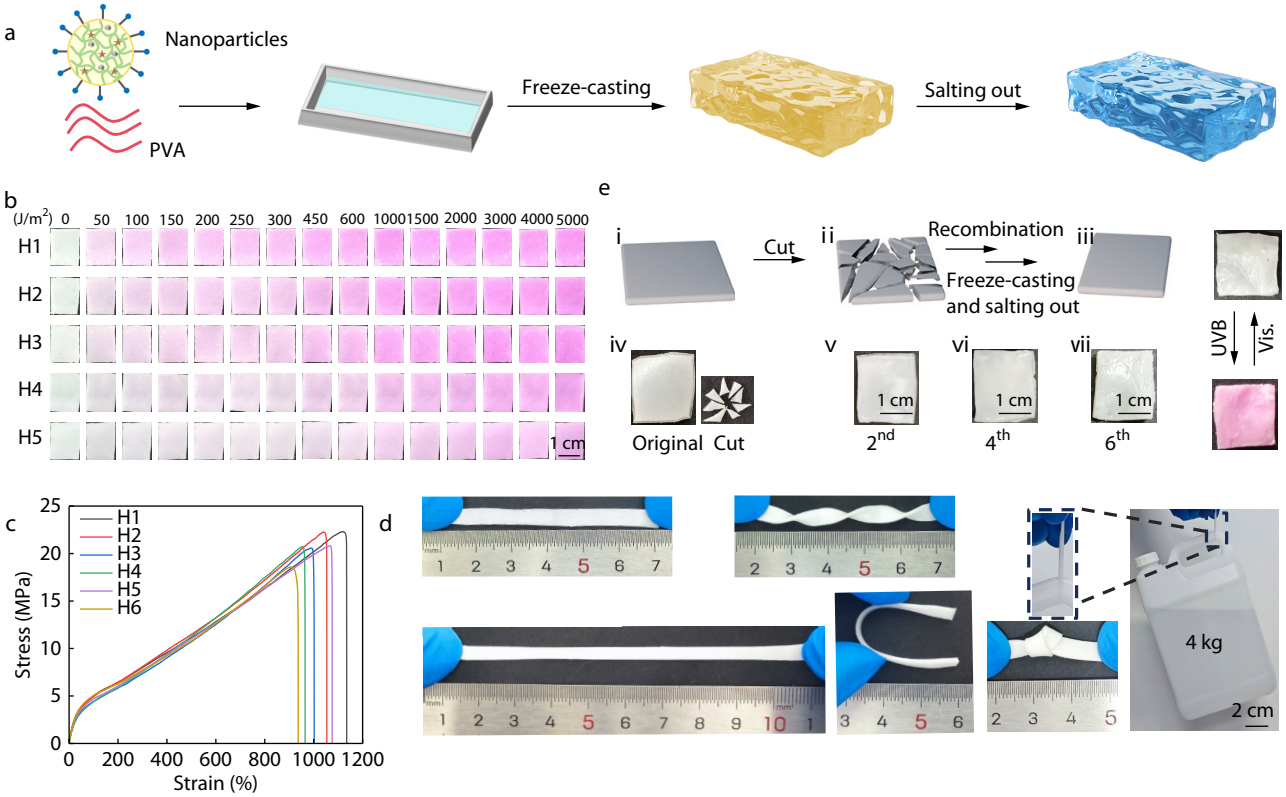
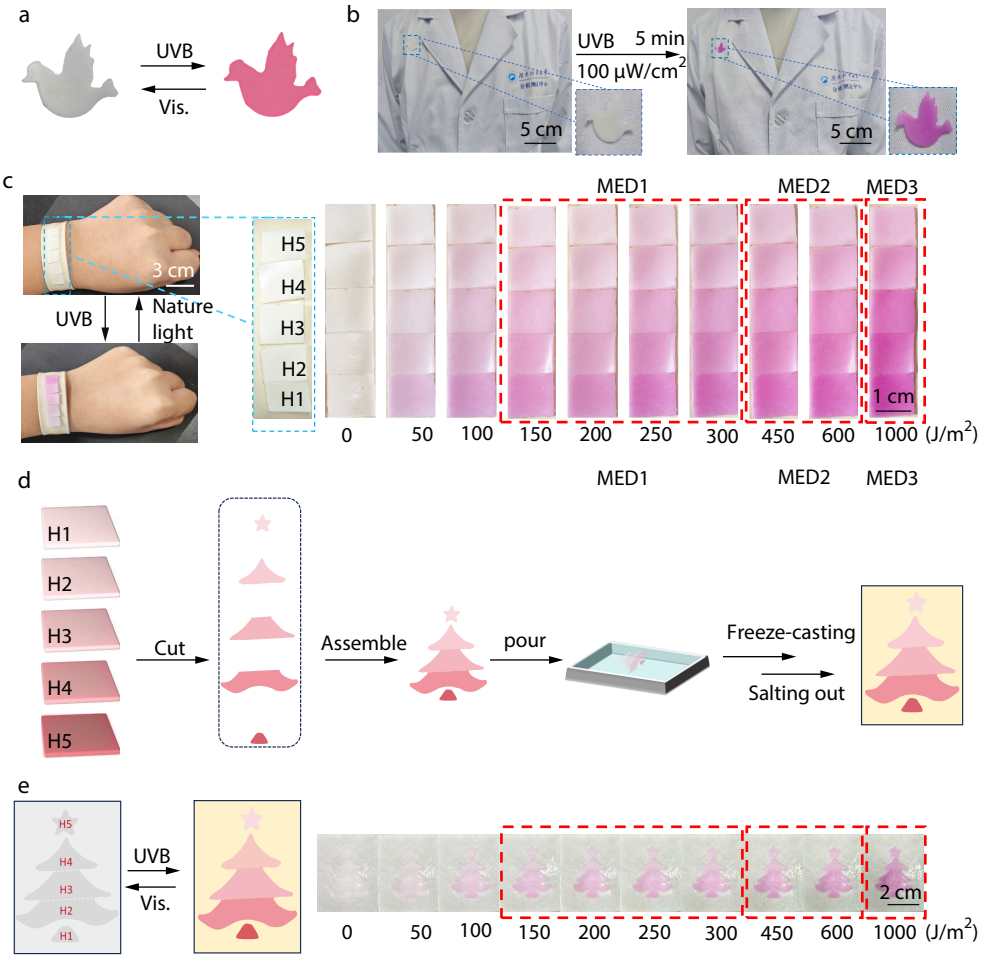


Fig. 4 (a) Schematic diagram of the preparation process of PHs; (b) The color change of hydrogels under UVB (302 nm) radiation (0–5000 J/m^2); (c) Stress-strain curves of H1–H6, H6 is the control sample without nanoparticles; (d) Mechanical properties of H1: virgin, twisting, stretching, curve, knotting, lifting a water bottle (4 kg); (e) Schematic illustration of recycling. (i) Original sample, (ii) chopped sample, and (iii) recyclable sample. Photographs of the original sample and chopped sample (iv, PHs-1), 2nd time (v, PHs-1-R), 4th time (vi, PHs-2-R), and 6th time (vii, PHs-3-R). Photographs of the recyclable sample (R1) after treating with Vis. (525 nm, 1.34 mW/cm^2) and UVB (302 nm, 100 μW/cm^2).

mixed with water to obtain a solid content of 17.6 wt% and dissolved at 90 °C to obtain a homogeneous viscous solution. Subsequently, the solution was poured into a glass mold with a spacing of 2 mm and subjected to three freeze-thaw cycles (–20 °C for 12 h and 25 °C for 12 h). Finally, the regenerated transparent hydrogel was immersed in a 1.5 mol/L sodium citrate solution for seven days to produce recycled samples after two, four, and six reprocessing cycles (Fig. 4e). Notably, repeated recycling had a negligible effect on the mechanical properties of the hydrogels, indicating their excellent reprocessability and structural robustness.

UVB Detection

Wearable devices have emerged as an important platform for continuous personal health monitoring and environmental protection, enabling real-time assessment of physiological status and harmful environmental exposures, such as ultraviolet radiation.[60–62] Hydrogels have attracted considerable attention as promising materials for wearable sensing applications because of their excellent biocompatibility, flexibility, and skin conformability. To demonstrate the applicability of the prepared hydrogels for wearable UV monitoring, a hydrogel (H1) was first cut into a dove-shaped pattern and attached to a piece of clothing (Figs. 5a and 5b). Upon exposure to UVB irradiation (302 nm), the pattern gradually changed from colorless to red, exhibiting a pronounced photochromic response (Figs. 5a and 5b). A wearable wristband was fabricated for UVB monitoring (Fig. 5c). The device consisted of a bistable snap wristband serving as the substrate and five hydrogel patches (H1–H5) containing different concentrations of Trz as the sensing units. Upon UVB exposure, the hydrogel patches exhibited distinct progressive photochromic responses (Fig. 5c). Specifically, the hydrogel with the lowest Trz content responded first, followed by the other hydrogels sequentially, resulting in stepwise color evolution. This behavior resulted from the competitive UV energy-harvesting mechanism between Trz and DTE, whereby increasing the Trz loading progressively increased the threshold UV dose required to activate the photochromic transition. Moreover, owing to the excellent reversibility of DTE, the colored hydrogels spontaneously reverted to their initial colorless state under ambient light conditions without requiring additional visible light irradiation. Consequently, the device can be repeatedly used through simple and user-friendly operation. Inspired by commercial indicator strips, hydrogel patches were arranged in a strip-like configuration to produce a sequential color change from bottom to top under UVB irradiation. The response thresholds of the hydrogel patches were designed to correspond to different levels of the minimum erythema dose (MED), thereby enabling gradient and semiquantitative detection of UVB exposure. Compared with conventional visual UV indicators that rely solely on variations in color intensity, the present strategy pro-



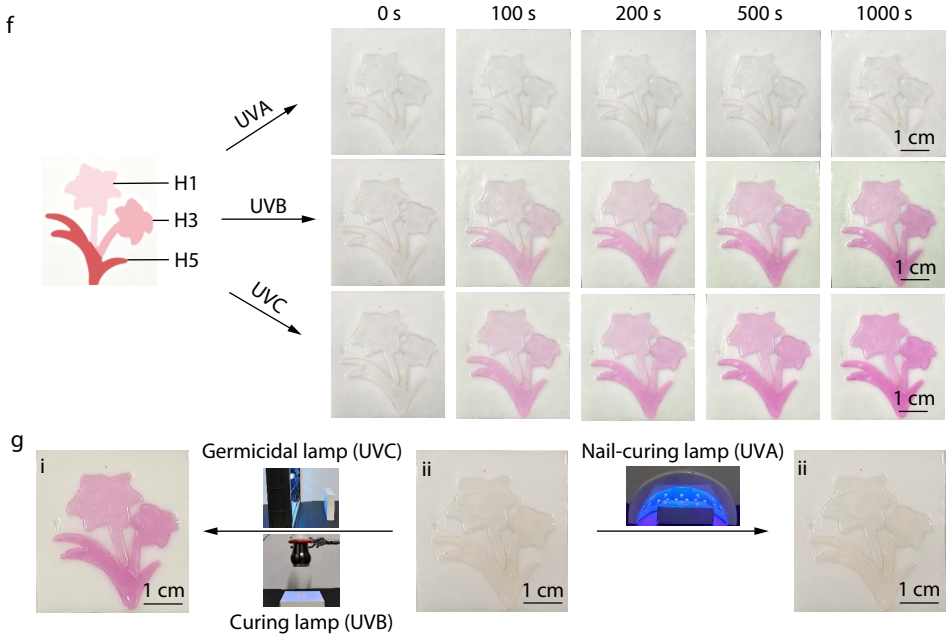


Fig. 5 The integrated single-platform for UVB detection. (a) Schematic diagram of photo-induced color change; (b) Photographs in wearable hydrogel label pasted on the laboratory coat before and after UVB irradiation (100 μW/cm^2); (c) Photographs of wearable hydrogel watches under UVB and nature light, and the corresponding photographs of color change of hydrogels under UVB radiation (0–1000 J/m^2); (d) Schematic diagram of preparation of integrated wearable devices based on "tree" using H1, H2, H3, H4, and H5; (e) Schematic diagram of photo-induced color change in integrated wearable devices based on "tree"; (f) Schematic diagram of integrated wearable devices based on "flower" prepared by H1, H3, and H5 and the corresponding photographs under UVA (365 nm, 15 mW/cm^2), UVB (302 nm, 100 μW/cm^2), and UVC (254 nm, 1 mW/cm^2) radiation for the different times (0–1000 s); (g) Photographs of integrated wearable devices based on "flower" under nail-curing devices (UVA, 365 nm, 1 mW/cm^2), industrial curing lamps (UVB, 302 nm, 100 μW/cm^2), and germicidal lamps (UVC, 254 nm, 100 μW/cm^2) irradiation for 10 min.

vided substantially improved resolution and contrast, allowing a more intuitive and accurate assessment of UVB exposure levels.

UVB detection can be achieved by simply combining the corresponding basic functional units (Fig. 5c), but the mechanical performance of the tough hydrogel still needs to be fully utilized. Therefore, we integrated different hydrogel units with programmable response thresholds into a single wearable platform (Fig. 5d). The integrated wearable devices based on "tree" prepared by H1, H2, H3, H4, and H5 can convert cumulative UVB exposure into discrete and highly distinguishable color states (Fig. 5e). The degree of color change decreased significantly as the concentration of Trz increased. This strategy provides an intuitive, high-resolution, and reusable approach for real-time personal UVB monitoring, and offers considerable potential for applications in skin photoprotection, outdoor health management, and intelligent wearable devices.

Although monitoring solar UVB is of primary importance, artificial UV sources are ubiquitous in daily life, including UVA from nail-curing devices, UVB from industrial curing lamps, and UVC from germicidal lamps. Therefore, the performance of the PHs was further evaluated in these representative irradiation environments. To visualize the wavelength-selective response, integrated "flower" patterns were fabricated by combining H1, H3, and H5 and subsequently exposed to UVA (365 nm), UVB (302 nm), and UVC (254 nm) irradiation. As shown in Fig. 5(f), the hydrogels exhibited negligible color variation under UVA exposure, whereas pronounced and programmable color evolution occurred within 1000 s under both UVB and UVC irradiation. To further demonstrate its practical applicability, commercially available nail-curing lamps (UVA), industrial curing lamps (UVB), and germicidal lamps (UVC) were used as irradiation sources (Fig. 5g). Consistent with the laboratory results, no obvious color change was observed under the nail-curing lamp, whereas distinct chromatic transitions were readily induced by both germicidal and curing lamps (Fig. 5g). These results confirm that the hydrogel could selectively detect UVB and UVC radiation from practical UV sources, while remaining insensitive to UVA interference. Collectively, the programmable color evolution of the individual hydrogel units under different ultraviolet wavelengths established a versatile platform for wavelength-selective ultraviolet sensing, environmental UV monitoring, and high-security optical warning applications.

Specifically, the integrated single-platform design eliminates the need for additional assembly and encapsulation, thereby simplifying the fabrication and minimizing interfacial defects. The intimate integration of the sensing components within the robust hydrogel matrix also improves mechanical integrity and prevents component displacement or delamination during deformation. More importantly, this architecture simultaneously integrates UV sensing, optical signal generation, and wearable functionality, thereby providing a compact, flexible, and reliable platform for real-time UV monitoring and anti-counterfeiting applications.

CONCLUSIONS

In summary, we described a wavelength-selective and mechanically robust photochromic hydrogel platform by integrating

https://doi.org/10.1007/s10118-026-3861-9

DTE/Trz-loaded polymer nanoparticles into PVA hydrogels through the synergy of freeze-casting and salting-out. The uniform nanoparticles retained the excellent photoresponsive characteristics of the diarylethene derivatives, including rapid photoswitching, outstanding reversibility, and long-term photostability. More importantly, the introduction of Trz established a competitive UV absorption mechanism with DTE, which effectively suppressed interference from UVA and enabled programmable UVB dose thresholds and graded color responses. The resulting PHs exhibited excellent toughness, high tensile strength (22.29 MPa), flexibility, load-bearing capability, environmental stability, and recyclability while preserving the photochromic performance of the nanoparticles. By integrating multiple hydrogel sensing units with programmable response thresholds into a wearable wristband, cumulative UVB exposure can be converted into discrete and visually distinguishable color states corresponding to different MED levels, enabling intuitive, high-resolution, and reusable UVB monitoring. Collectively, the integration of UV-absorbing and photochromic components establishes a competitive energy-harvesting mechanism, enabling programmable and visually distinguishable responses to different UVB dose ranges, and provides a versatile platform for high-resolution ultraviolet dosimetry and practical optical warning applications.

Conflict of Interests

The authors declare no interest conflict.

Electronic Supplementary Information

Electronic supplementary information (ESI) is available free of charge in the online version of this article at http://doi.org/10.1007/s10118-026-3861-9.

Data Availability Statement

The related data of this paper is data that should not be shared, and can be obtained from the author for reasonable reasons. Contact information: whgxily@gmail.com (H. W.) and cj0066@gmail.com (J. C.).

ACKNOWLEDGMENTS

The work was financially supported by the National Natural Science Foundation of China (Nos. 52273206 and 52403266), National Key R&D Program of China (Nos. 2023YFB3812400 and 2023YFB3812403), Hainan Provincial Natural Science Foundation of China (No. 526MS0237), and Scientific Research Fund of Hunan Provincial Education Department (No. 25A0371).

REFERENCES

1 Bogh, M. K. B. Vitamin D production after UVB: aspects of UV-related and personal factors. *Scand. J. Clin. Lab. Investig.* **2012**, *72*, 24–31.
2 Armstrong, B. K.; Kricker, A. The epidemiology of UV induced skin cancer. *J. Photochem. Photobiol. B Biol.* **2001**, *63*, 8–18.
3 Yang, T. T.; Lan, C. E. Photocarcinogenesis of the skin: current status and future trends. *Kaohsiung J. Med. Sci.* **2025**, *41*, e12946.
4 Nishisgori, C. Current concept of photocarcinogenesis. *Photochem. Photobiol. Sci.* **2015**, *14*, 1713–1721.
5 Yam, J. C. S.; Kwok, A. K. H. Ultraviolet light and ocular diseases. *Int. Ophthalmol.* **2014**, *34*, 383–400.
6 Young, A. R. Acute effects of UVR on human eyes and skin. *Prog. Biophys. Mol. Biol.* **2006**, *92*, 80–85.
7 Salminen, A.; Kaarniranta, K.; Kauppinen, A. Photoaging: UV radiation-induced inflammation and immunosuppression accelerate the aging process in the skin. *Inflamm. Res.* **2022**, *71*, 817–831.
8 Huang, Y.; Ning, L.; Zhang, X.; Zhou, Q.; Gong, Q.; Zhang, Q. Stimuli-fluorochromic smart organic materials. *Chem. Soc. Rev.* **2024**, *53*, 1090–1166.
9 Klajn, R. Spiropyran-based dynamic materials. *Chem. Soc. Rev.* **2014**, *43*, 148–184.
10 Wang, H.; Tian, Y.; Wu, T.; He, S.; Cui, J.; Chen, J.; Chen, X. Photoswitchable dual-color fluorescent polymeric nanoparticles for self-erased time-resolved information encryption and anti-counterfeiting. *Chin. Chem. Lett.* **2025**, *36*, 110509.
11 Wang, H.; Deng, H.; Chen, J.; Tian, Y.; Huang, F.; Zhao, Y.; Zhou, Z.; Cui, J.; Chen, J.; Chen, X. Self-growth of programmable 2D- and 3D-coupling responsive coating for anti-counterfeiting. *Nat. Commun.* **2026**, *17*, 1009.
12 Gao, A.; Sun, F.; Duan, Y.; Zhang, Y.; Liu, X.; Liu, T.; Ji, Y.; Wu, Q.; Deng, X.; Zheng, Y.; Wei, C.; Wang, D. Programmable encryption based on photochromism of spiropyrans and donor–acceptor stenhouse adducts. *Adv. Funct. Mater.* **2024**, *34*, 2316457.
13 Yang, X.; Du, M.; Chu, Z.; Li, C. Synchronizing multicolor changes and shape deformation into structurally homogeneous hydrogels *via* a single photochromophore. *Adv. Mater.* **2025**, *37*, 2500857.
14 Wang, Q.; Lin, B.; Chen, M.; Zhao, C.; Tian, H.; Qu, D. H. A dynamic assembly-induced emissive system for advanced information encryption with time-dependent security. *Nat. Commun.* **2022**, *13*, 4185.
15 Irie, M.; Fukaminato, T.; Matsuda, K.; Kobatake, S. Photochromism of diarylethene molecules and crystals: memories, switches, and actuators. *Chem. Rev.* **2014**, *114*, 12174–12277.
16 Irie, M. Diarylethenes for memories and switches. *Chem. Rev.* **2000**, *100*, 1685–1716.
17 Irie, M. Photochromism of diarylethene single molecules and single crystals. *Photochem. Photobiol. Sci.* **2010**, *9*, 1535–1542.
18 Li, R.; Ou, T.; Wen, L.; Yan, Y.; Li, W.; Qin, X.; Wang, S. All-visible-light-activated diarylethene photoswitches. *Molecules* **2024**, *29*, 5202.
19 Li, Z.; Zeng, X.; Gao, C.; Song, J.; He, F.; He, T.; Guo, H.; Yin, J. Photoswitchable diarylethenes: from molecular structures to biological applications. *Coord. Chem. Rev.* **2023**, *497*, 215451.
20 Jiang, J.; Chen, Q.; Xu, M.; Chen, J.; Wu, S. Photoresponsive diarylethene-containing polymers: recent advances and future challenges. *Macromol. Rapid Commun.* **2023**, *44*, 2300117.
21 Ai, Q.; Lan, K.; Li, L.; Liu, Z.; Hu, X. Beyond photochromism: alternative stimuli to trigger diarylethenes switching. *Adv. Sci.* **2024**, *11*, 2410524.
22 Xiang, H.; Liu, H.; Xu, X.; Lin, Z.; Wu, J.; Ye, T.; Huang, F.; Wang, H.; Zheng, Y.; Chen, J. Transparent, elastic and self-healable photochromic polymers for wearable UV detector. *J. Photochem. Photobiol. A Chem.* **2026**, *479*, 117282.
23 Bag, S. K.; Pal, A.; Jana, S.; Thakur, A. Recent advances on diarylethene-based photoswitching materials: applications in bioimaging, controlled singlet oxygen generation for photodynamic therapy and catalysis. *Chem.* **2024**, *19*,

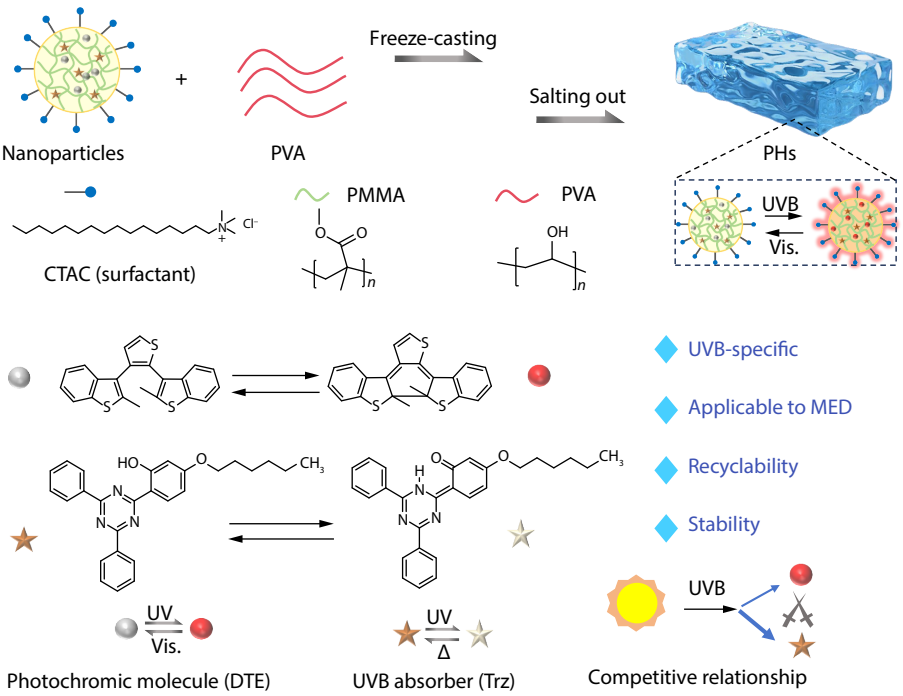
Graphical Abstract

Wavelength-selective Tough and Recyclable Photochromic Hydrogels Based on Competitive UV Energy Harvesting for Specific UVB Detector

Ting Ye, Hai-Bo Xiang, Meng-Xia Huang, Zi-Yuan Zhang, Kai-Rong Zang, Hong Wang, and Jian Chen

Hunan University of Science and Technology; Sanya Institute of Hunan University of Science and Technology

A competitive UV energy-harvesting strategy was established by integrating Ultraviolet B (UVB) absorbers and diarylethene photochromic units into tough poly(vinyl alcohol) (PVA) hydrogels, enabling wavelength-selective, dose-resolved, and mechanically robust visual UVB sensing for wearable monitoring.



Chinese J. Polym. Sci. 2026 *https://doi.org/10.1007/s10118-026-3861-9*

e202400238.

24 Wiedbrauk, S.; McKinnon, H.; Swann, L.; Boase, N. R. B. Diarylethene photoswitches and 3D printing to fabricate rewearable colorimetric UV sensors for Sun protection. *Adv. Mater. Technol.* **2023**, *8*, 2201918.

25 Hassan, S. Z.; Song, J.; Yu, S. H.; Chung, D. S. Critical factors of diarylethene for a high-performance photoprogrammable polymer transistor: crystallographic compatibility, quantum yield, and fatigue resistance. *Chem. Mater.* **2021**, *33*, 7546–7557.

26 Miyamoto, R.; Kitagawa, D.; Kobatake, S. Fatigue resistance of photochromic diarylethene in the presence of cyclodextrins with different pore sizes. *Bull. Chem. Soc. Jpn.* **2022**, *95*, 639–645.

27 Hassan, S. Z.; Yu, S. H.; So, C.; Moon, D.; Chung, D. S. End-functionalization of diarylethene for opto-electronic switching with high fatigue resistance. *Chem. Mater.* **2021**, *33*, 403–412.

28 Zou, J.; Liao, J.; He, Y.; Zhang, T.; Xiao, Y.; Wang, H.; Shen, M.; Yu, T.; Huang, W. Recent development of photochromic polymer systems: mechanism, materials, and applications. *Research* **2024**, *7*, 0392.

29 Zou, W.; González, A.; Jampaiah, D.; Ramanathan, R.; Taha, M.; Walia, S.; Sriram, S.; Bhaskaran, M.; Dominguez-Vera, J. M.; Bansal, V. Skin color-specific and spectrally-selective naked-eye dosimetry of UVA, B and C radiations. *Nat. Commun.* **2018**, *9*, 3743.

30 Caetano, M.; Gregório, J.; Paulo, M. S. Analyzing the reliability and cost of the most commonly used dosimeters for personal ultraviolet radiation monitoring—a rapid review. *Atmosphere* **2024**, *15*, 1531.

31 Fanselow, D. L.; Pathak, M. A.; Crone, M. A.; Ersfeld, D. A.; Raber, P. B.; Trancik, R. J.; Dahl, M. V. Reusable ultraviolet monitors: design, characteristics, and efficacy. *J. Am. Acad. Dermatol.* **1983**, *9*, 714–723.

32 Zou, W.; Sastry, M.; Gooding, J. J.; Ramanathan, R.; Bansal, V. Recent advances and a roadmap to wearable UV sensor technologies. *Adv. Mater. Technol.* **2020**, *5*, 1901036.

33 Zhang, X.; Li, X.; Lang, Y.; Wu, P. Low-cost naked-eye UVB and UVC dosimetry based on 3, 3′, 5, 5′-tetramethylbenzidine. *Anal. Chem.* **2022**, *94*, 4373–4379.

34 Monteiro, B.; Leal, J. P.; Outis, M.; Casimiro, M. H.; Pereira, C. C. L. Irradiation-responsive polysulfone film as a colorimetric UVA/UVB differentiator. *J. Mater. Chem. C* **2023**, *11*, 5199−5207.
35 Wen, G. Y.; Zhou, X.L.; Tian, X. Y.; Hu, T. Y.; Xie, R.; Ju, X. J.; Liu, Z.; Pan, D. W.; Wang, W.; Chu, L. Y. Real-time quantitative detection of ultraviolet radiation dose based on photochromic hydrogel and photo-resistance. *Chem. Mater.* **2022**, *34*, 7947−7958.
36 Yang, Y.; Guan, L.; Jiang, H.; Duan, L.; Gao, G. A rapidly responsive photochromic hydrogel with high mechanical strength for ink-free printing. *J. Mater. Chem. C* **2018**, *6*, 7619−7625.
37 Hu, W.; Ejeromedoghene, O.; Xia, Y.; Fu, G. A multi-functional and rapid responsive photochromic hydrogel for UV indicators. *Macromol. Chem. Phys.* **2021**, *222*, 2000427.
38 Lu, H.; Huang, H.; Yang, J.; Zheng, Z.; Dong, X.; Zhao, L.; Xu, C.; Hu, J.; Liu, H.; Qian, Y.; Wang, J. Q.; Lin, J. Incorporating photochromic viologen derivative to unprecedentedly boost UV sensitivity in photoelectrochromic hydrogel. *ACS Sens.* **2023**, *8*, 1609−1615.
39 Yang, Z.; Hu, J.; Van der Heggen, D.; Jiao, M.; Feng, A.; Vrielinck, H.; Smet, P. F.; Poelman, D. A versatile photochromic dosimeter enabling detection of X-ray, ultraviolet, and visible photons. *Laser Photonics Rev.* **2023**, *17*, 2200809.
40 Shi, H.; Wang, X.; Guo, H.; Yang, Y.; Yang, Y. Antiswelling photochromic hydrogels for underwater optically camouflageable flexible electronic devices. *ACS Appl. Mater. Interfaces* **2024**, *16*, 46810−46821.
41 Zhang, R.; Chen, Y.; Liu, Y. Light-driven reversible multicolor supramolecular shuttle. *Angew. Chem. Int. Ed.* **2023**, *62*, e202315749.
42 Wu, Y. G.; Zhou, W. L.; Qiu, Y.; Wang, S.; Liu, J.; Chen, Y.; Xu, X.; Liu, Y. 4D assembly of time-dependent lanthanide supramolecular multicolor phosphorescence for encryption and visual sensing. *Adv. Sci.* **2025**, *12*, 2415418.
43 Wang, H.; He, S.; Chen, F.; Tian, Y.; Li, X.; Chen, J.; Huang, F.; Cui, J.; Chen, J. Micelles-assisted strengthening of tough photoswitchable fluorescent hydrogels for recyclable information encryption and anti-counterfeiting. *Adv. Mater. Technol.* **2026**, *11*, e02046.
44 Zhu, M. Q.; Zhu, L.; Han, J. J.; Wu, W.; Hurst, J. K.; Li, A. D. Q. Spiropyran-based photochromic polymer nanoparticles with optically switchable luminescence. *J. Am. Chem. Soc.* **2006**, *128*, 4303−4309.
45 Kim, D.; Jeong, K.; Kwon, J. E.; Park, H.; Lee, S.; Kim, S.; Park, S. Y. Dual-color fluorescent nanoparticles showing perfect color-specific photoswitching for bioimaging and super-resolution microscopy. *Nat. Commun.* **2019**, *10*, 3089.
46 Hua, M.; Wu, S.; Ma, Y.; Zhao, Y.; Chen, Z.; Frenkel, I.; Strzalka, J.; Zhou, H.; Zhu, X.; He, X. Strong tough hydrogels *via* the synergy of freeze-casting and salting out. *Nature* **2021**, *590*, 594−599.
47 Pang, Z.; Li, S.; Si, M.; Chen, Y.; He, P.; Zhang, C. W.; Du, C.; Han, X.; Wei, M.; He, X.; Liu, H. Amplified friction *via* a cooperative entanglement domains and steric hindrance for damping hydrogels. *Nat. Commun.* **2026**, *17*, 6956.
48 Shi, P.; Si, M.; Lin, Z.; Mao, Q.; Duan, S.; Liu, Z.; Hong, W.; Possinger, M.; Yan, Y.; Chen, C.; He, P.; Zuo, X.; Zhou, H.; van Duin, A.; He, X. Harnessing chain mobility *via* protonation for tough and isotropic hydrogel. *Adv. Mater.* **2026**, *38*, e17407.
49 Sun, J. Y.; Zhao, X.; Illeperuma, W. R. K.; Chaudhuri, O.; Oh, K. H.; Mooney, D. J.; Vlassak, J. J.; Suo, Z. Highly stretchable and tough hydrogels. *Nature* **2012**, *489*, 133−136.
50 Liang, X.; Zhong, H. J.; Ding, H.; Yu, B.; Ma, X.; Liu, X.; Chong, C. M., He, J. Polyvinyl alcohol (PVA)-based hydrogels: recent progress in fabrication, properties, and multifunctional applications. *Polymers* **2024**, *16*, 2755.
51 Lei, D.; Xiao, Y.; Han, Y.; Yang, H. Y.; Xi, M.; Jiang, Y.; Li, Y. Dual-stimuli-responsive, anti-freezing, and conductive ionic hydrogels for smart wearable and outdoor UV radiation monitoring devices. *Sens. Actuators A Phys.* **2024**, *366*, 114978.
52 Xia, H.; Wu, Z.; Tang, Q.; Yang, Z. Dual-response UV radiation detector based on color switching and photoresistance response for UV radiation monitoring. *ACS Appl. Mater. Interfaces* **2025**, *17*, 5382−5390.
53 Sun, A.; Nan, F.; Wei, Q.; Wang, L.; Yu, W. W. Color-tunable, multifunctional photochromic composites for wearable UV monitoring and biomechanical energy harvesting. *Nano Energy* **2024**, *126*, 109679.
54 Zhao, Y.; Ran, B.; Lee, D.; Liao, J. Photo-controllable smart hydrogels for biomedical application: a review. *Small Meth.* **2024**, *8*, 2301095.
55 Wang, X.; Ji, H.; Gao, L.; Hao, R.; Shi, Y.; Yang, J.; Hao, Y.; Chen, J. Wearable hydrogel-based health monitoring systems: a new paradigm for health monitoring. *Chem. Eng. J.* **2024**, *495*, 153382.
56 Yimyai, T.; Crespy, D.; Pena-Francesch, A. Self-healing photochromic elastomer composites for wearable UV-sensors. *Adv. Funct. Mater.* **2023**, *33*, 2213717.
57 Paterson, M. J.; Robb, M. A.; Blancafort, L.; DeBellis, A. D. Mechanism of an exceptional class of photostabilizers: a seam of conical intersection parallel to excited state intramolecular proton transfer (ESIPT) in *o*-hydroxyphenyl-(1,3,5)-triazine. *J. Phys. Chem. A* **2005**, *109*, 7527−7537.
58 Wang, J.; Jeevarathinam, A. S.; Jhunjhunwala, A.; Ren, H.; Lemaster, J.; Luo, Y.; Fenning, D. P.; Fullerton, E. E.; Jokerst, J. V. A wearable colorimetric dosimeter to monitor sunlight exposure. *Adv. Mater. Technol.* **2018**, *3*, 1800037.
59 Kundu, S.; Jaggernauth, A.; O'Connor, R.; Vijayaraghavan, R. K. A dual-mode photoconductive colorimetric wearable UV-dosimeter: strategies for tunable UV-band sensitivity. *Small* **2026**, *22*, e74441.
60 Suryaprabha, T.; Choi, C.; Wu, Y.; Liu, L., Hwang, B. Smart wearable and implantable biosensors for continuous health monitoring: materials, biocompatibility, and AI integration. *npj Flex. Electron.* **2026**, *10*, 46.
61 Vaghasiya, J. V.; Mayorga-Martinez, C. C.; Pumera, M. Wearable sensors for telehealth based on emerging materials and nanoarchitectonics. *npj Flex. Electron.* **2023**, *7*, 26.
62 Xue, Z.; Gai, Y.; Wu, Y.; liu, Z.; Li, Z. Wearable mechanical and electrochemical sensors for real-time health monitoring. *Commun. Mater.* **2024**, *5*, 211.

https://doi.org/10.1007/s10118-026-3861-9